View Article Online / Journal Homepage / Table of Contents for this issue
Dynamic Article Links

ChemComm

Cite this: *Chem. Commun.*, 2011, **47**, 4658–4660

www.rsc.org/chemcomm

COMMUNICATION

Sterically congested, hexameric tetra*kis*pyridinyl-Pd^{II}/Cd^{II}-metallomacrocycles: self-assembly and structural characterization†

Sujith Perera,[a] Xiaopeng Li,[b] Mingming Guo,[a] Chrys Wesdemiotis,*[ab] Charles N. Moorefield[a] and George R. Newkome*[ab]

Received 1st February 2011, Accepted 23rd February 2011
DOI: 10.1039/c1cc10649j

Published on 17 March 2011. Downloaded by Michigan State University on 21/01/2016 22:52:55.

Hexagonal Pd^{II}- or Cd^{II}-tetra*kis*pyridinyl-based macrocycles are quantitatively self-assembled from 4′-(3-pyridinyl)-4,4′′-di(*tert*-butyl)-2,2′:6′,2′′-terpyridine and structurally confirmed by NMR and TWIM-MS.

Self-assembly procedures have been elegantly used to construct diverse 2D and 3D macromolecular architectures.[1] Among these self-assembly processes, inorganic metal coordination has played a pivotal role[2] and instilled important utilitarian electronic, catalytic, photophysical, and magnetic properties.[3] Tridentate terpyridine-metal coordination has been successfully used to assemble diverse metallomacrocycles generating boxes, helixes, and other polygonal shapes.[4] Similarly, *bis*terpyridinyl ligands possessing 60–120° angles between the two ligating termini, have been shown to self-assemble into various metallomacromolecules.[5] Designing tridentate and monodentate coordination sites within the same ligand along with tunable directionality provides an opportunity to utilize stronger and weaker coordination sites for the assembly of new polygons.

Under mild ionization conditions, ESI-MS has been used in the identification and characterization of supramolecules.[6–9] Unfortunately, the peaks from different charge states are known to superimpose; even with the high resolving power of Fourier Transform Mass Spectrometry (FTMS), only a few isotope patterns of different charge states have been deconvoluted.[7] Recently, traveling wave ion mobility mass spectrometry (TWIM-MS)[10] and traditional IM-MS[11] have been employed in the detection and characterization of complex metallomacrocycles.[12] This technique alleviates isomer superposition and deconvolutes the isotope patterns of differently charged ions, which significantly facilitates structure elucidation. Combining molecular modeling and 2D diffusion ordered NMR spectroscopy (DOSY) experiments, with TWIM-MS data affords complementary and reliable structural information.

Herein, we report the self-assembly of hexagonal Pd^{II}- or Cd^{II}-polypyridinyl-based macrocycles using both mono- and tridentate coordination sites. Hexagonal macrocyclic formation from a one-pot reaction is confirmed from ^{1}H and ^{13}C NMR, 2D COSY NMR, and TWIM-MS methods. Moreover, hydrodynamic radii obtained from DOSY NMR are in accord with radii calculated from preliminary molecular modeling and the drift time trends observed TWIM-MS data.

In order to enhance the solubility and ascertain the issues associated with potential steric hindrance, the synthesis of 4′-(3-pyridinyl)-4,4′′-di(*tert*-butyl)-2,2′:6′,2′′-terpyridine (**1**) was undertaken (Scheme 1). Acetylation of 4-*tert*-butylpyridine[13] in the 2-position generated the previously prepared[14,15] precursor 4-*tert*-butyl-2-acetylpyridine; however, our one-pot acetylation of 4-*tert*-butylpyridine leads to a higher yield and enhanced purity. The desired ligand **1** was prepared using a modified procedure for 4′-(3-pyridinyl)-2,2′:6′,2′′-terpyridine[16] based on sequential addition of 4-*tert*-butyl-2-acetylpyridine (see Scheme S1†). The ^{1}H NMR spectra of **1** showed the presence of singlet peaks at δ 9.14 (s, H^{a}), 8.79 (s, Py$H^{3',3''}$), 8.71 (s, Py$H^{3',5''}$) (see Fig. 1) and 1.48 [s, C(CH_3)]; the proper peak assignments were confirmed using two-dimensional 2D COSY NMR. ^{13}C NMR and ESI-MS spectra also supported the structure of **1**: $(m/z) = 423.2\ [M+H]^{+}$ (calcd $m/z = 423.2$).

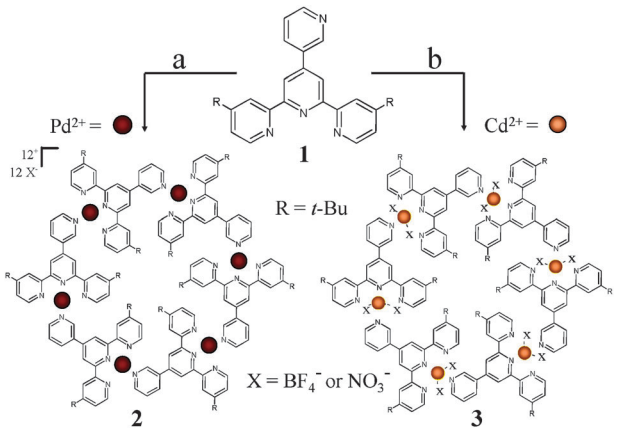

Scheme 1 Self-assembly of the macrocyclic palladium (**2**) and cadmium (**3**) hexamers: (a) MeCN, $Pd(MeCN)_4(BF_4)_2$, 24 h, 60 °C; (b) $CDCl_3$/CD_3OD (3 : 2), $Cd(NO_3)_2{\cdot}4H_2O$, 5 min., 25 °C.

[a] *Department of Polymer Science, The University of Akron, Akron, OH 44325-4717, USA. E-mail: newkome@uakron.edu, wesdemiotis@uakron.edu; Fax: +1 330-972-2413; Tel: +1 330-972-6458*
[b] *Department of Chemistry, The University of Akron, Akron, OH 44325-3601, USA*

† Electronic supplementary information (ESI) available: Detailed experimental procedures with analytical data. See DOI: 10.1039/c1cc10649j

This journal is © The Royal Society of Chemistry 2011

View Article Online

Published on 17 March 2011. Downloaded by Michigan State University on 21/01/2016 22:52:55.

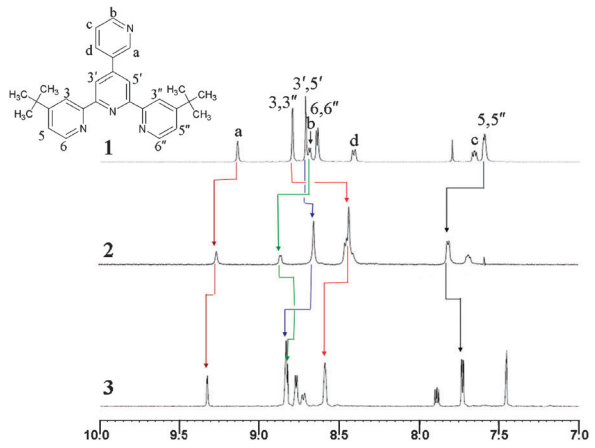

Fig. 1 The ^{1}H NMR of ligand **1** and complexes **2** and **3** showing aromatic regions (**1** in $CDCl_3/CD_3OD$, **2** in CD_3CN, **3** in $CDCl_3/CD_3OD$).

The polydentate ligand **1** possessing two unique, 120° angularly juxtaposed coordination sites was treated with one equivalent of either $[Pd(MeCN)_4(BF_4)_2]$ in MeCN or $Cd(NO_3)_2{\cdot}4H_2O$ in $CDCl_3:CD_3OD$ (3 : 2) to give the hexametallic macromolecules $[Pd_6(\mathbf{1})_6(BF_4)_{12}]$ (**2**) and $[Cd_6(\mathbf{1})_6(NO_3)_{12}]$ (**3**), respectively, in quantitative yields (Scheme 1). ^{1}H NMR data established the formation of a single type of tridentate terpyridine coordination with either Pd^{II} or Cd^{II} with absorptions at δ 8.65_{Pd} (s, tpy$H^{3',5'}$) or 8.59_{Cd} (s, tpy$H^{3,3''}$) and δ 7.81_{Pd} or 7.74_{Cd} (d, tpy$H^{5,5''}$). The downfield shifts of H^a singlet signal [from δ 9.14 to 9.26_{Pd}, ($\Delta\delta$ = 0.12) or δ 9.33_{Cd} ($\Delta\delta$ = 0.19)] and the H^b doublet signal [from δ 8.69 to 8.86_{Pd}, ($\Delta\delta$ = 0.17) or δ 8.83_{Cd} ($\Delta\delta$ = 0.14)] support the coordination of monodentate pyridine unit to the metal center (see Fig. 1). Sharp singlets assigned to the $C(CH_3)_3$ moieties ($\delta_{Pd/Cd}$ = 1.47) for **2** and **3**, along with a single type of metal-coordinated terpyridine unit in each macrocycle are indicative of the formation of symmetric, cyclic structures. The hexameric sizes were validated by ESI-MS: macrocycle **2** gave rise to signals at *m*/*z* 2023 $[6L+6Pd+10BF_4]^{2+}$, 1987 $[6L+6Pd+9BF_4+1F]^{2+}$ (-1 BF_3), 1320 $[6L+6Pd+9BF_4]^{3+}$, and 1297 $[6L+6Pd+8BF_4+1F]^{3+}$ (-1 BF_3); whereas, macrocycle **3** showed peaks at *m*/*z* 1915 $[6L+6Cd+10NO_3]^{2+}$ and 1256 $[6L+6Cd+9NO_3]^{3+}$. Notably, the symmetry observed in the ^{1}H and ^{13}C NMR spectra further corroborated the formation of cyclic structures; 2D COSY NMR confirmed each of the ^{1}H NMR peak assignments.

Full mass spectra of both Pd^{II} and Cd^{II} metallomacrocycles are given in Fig. S3 and S4,† respectively. Corresponding spectra consist of different charge states of the hexameric metallomacrocycle and its linear fragments. The fragmentation of metal–ligand complexes in ESI is well-documented.[9,12a,c] All possible combinations of fragments for complexes **2** and **3** with different *m*/*z* values, due to the loss of counterions are given in Tables S1 and S2.† Table S3 shows different *m*/*z* values generated by further loss of neutral BF_3 units from complex **2** ions. In both macrocycles, the complete absence of unique *m*/*z* signals for pentameric and heptameric species provided additional support that the NMR-detected symmetric structures were hexameric. In both mass spectra, highly abundant signals can be observed at low *m*/*z*, due to possible overlap of the differently charged species with their linear fragments generated during ESI; therefore, TWIM-MS was conducted on **2** and **3** to prove the existence of the cyclic hexameric structure.

The ions possible at *m*/*z* 1320 from **2** are $[2L+2Pd+3BF_4]^{+}$, $[4L+4Pd+6BF_4]^{2+}$, and $[6L+6Pd+9BF_4]^{3+}$. Note that $[6L+6Pd+9BF_4]^{3+}$ could be linear or cyclic. After ion mobility separation, four species are detected at 4.50, 2.89, 1.99, and 1.71 ms, respectively (Fig. 2). The composition of each peak with unique drift time was determined from the corresponding isotope distribution and spacing.[12a–c] For instance, due to their isotope spacing of 0.33 amu, both the signals at 1.71 and 1.99 ms were assigned to $[6L+6Pd+9BF_4]^{3+}$. In the mobility separation, compact ions drift faster, while more extended ions drift more slowly. Thus, the peaks at 1.71 and 1.99 ms correspond to cyclic and linear ions of $[6L+6Pd+9BF_4]^{3+}$, respectively. The linear $[6L+6Pd+9BF_4]^{3+}$ ions could be generated by ring-opening of cyclic structure **2**, either in the ESI source or during IM separation, and further fragmentation could lead to the signals at 2.89 and 4.50 ms, corresponding to $[4L+4Pd+6BF_4]^{2+}$ and $[2L+2Pd+3BF_4]^{+}$, respectively. Losses of neutral BF_3 were observed from each charge state (see Table S3† for resulting *m*/*z* values from hexamer **2**). The pattern of BF_3 losses further confirms the charge state and composition assigned to each signal.

The ions at *m*/*z* 2023 from **2** were also selected for ion mobility separation (Fig. S5†). Analysis of the corresponding isotope patterns reveals the presence of three charge states at *m*/*z* 2023, having spacing of Δm = 1 (8.39 ms), 0.5 (4.78 ms), and 0.33 (3.52 ms) amu, corresponding to $[3L+3Pd+5BF_4]^{1+}$, $[6L+6Pd+10BF_4]^{2+}$, and $[9L+9Pd+15BF_4]^{3+}$, respectively. The only doubly charged species is assigned to the cyclic $[6L+6Pd+10BF_4]^{2+}$ hexamer.[12a,c] No linear component is detected for the 2+ ions, presumably because the additional BF_4^- counterion (as compared to the 3+ ions) enhances the stability of the macrocyclic structure, thus increasing the energy needed for ring-opening. The ions of $[9L+9Pd+15BF_4]^{3+}$

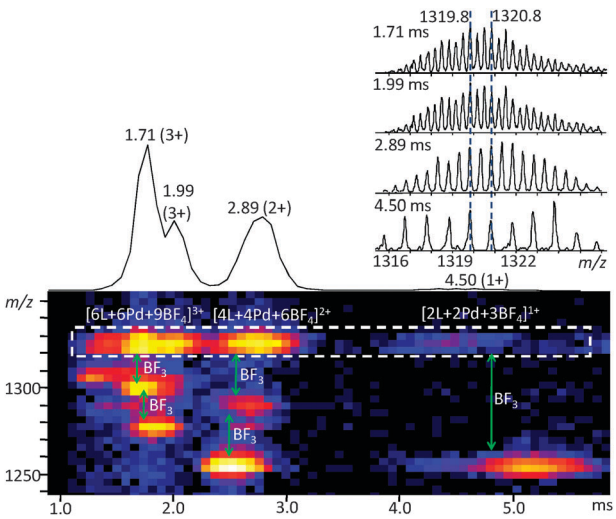

Fig. 2 Two-dimensional ESI-TWIM-MS plot for *m*/*z* 1320 from **2**. Ion mobility separation gave signals at 4.50, 2.89, 1.99, and 1.71 ms, corresponding to linear $[2L+2Pd+3BF_4]^{1+}$, linear $[4L+4Pd+6BF_4]^{2+}$, linear $[6L+6Pd+9BF_4]^{3+}$, and cyclic $[6L+6Pd+9BF_4]^{3+}$, respectively. The pattern of BF_3 losses observed from each species agrees well with the assigned charge state.

View Article Online

Published on 17 March 2011. Downloaded by Michigan State University on 21/01/2016 22:52:55.

could be a cluster of low charge states, such as the combination of $[3L + 3Pd + 5BF_4]^{1+}$ and $[6L + 6Pd + 10BF_4]^{2+}$; similar clusters were also observed in previous studies.[12a,c]

The ion mobility separation of m/z 1915 from **3** gave rise to three species, corresponding to $[3L + 3Cd + 5NO_3]^{1+}$, $[6L + 6Cd + 10NO_3]^{2+}$, and $[9L + 9Cd + 15NO_3]^{3+}$ appearing at 8.66, 4.78, and 3.70 ms, respectively (Fig. S6†). The cyclic $[6L + 6Cd + 10NO_3]^{2+}$ of **3** drifted at the same time (4.78 ms) as the cyclic $[6L + 6Pd + 10BF_4]^{2+}$ (Fig. S5†). Notably from **3**, there is a complete absence of the linear $[6L + 6Cd + 10NO_3]^{2+}$ isomer.

The DOSY NMR spectra of metallomacrocycles **2** and **3** clearly show the presence of only one species in solution for each. The experimental hydrodynamic radius (r_H), calculated *via* the Stokes–Einstein equation for each complex, is in excellent agreement with the mean radii obtained from the respective calculated structures (Table S4†). The DOSY NMR data unambiguously reveal that these self-assembled complexes have uniform macrocyclic architectures. The UV-vis and photoluminescence data for the ligand and complexes are also shown in the supporting information (Fig. S7 and Table S5†).

In conclusion, the self-assembled, hexameric, Pd^{II}- and Cd^{II}-polypyridine macrocycles **2** and **3** have been generated by taking advantage of the novel *bis*-functional ligand, 4′-(3-pyridinyl)-4,4′′-di(*tert*-butyl)-2,2′ : 6′,2′′-terpyridine. These hexameric Pd^{II} and Cd^{II} metallomacrocycles **2** and **3** were characterized using ^1H and ^{13}C NMR, 2D DOSY NMR, TWIM-MS, and molecular modeling. TWIM-MS completely deconvolutes the isotope patterns of different charge states, which avoids the isomer superposition prevalent in regular ESI-MS and FTMS. Further, the solution-phase hydrodynamic radii obtained by DOSY NMR are in full accord with the values predicted by molecular modeling.

The authors gratefully acknowledge support from the National Science Foundation (GRN: DMR-0812337, DMR-0705015, CW: DMR-0821313, CHE-1012636).

Notes and references

1 J.-M. Lehn, in *Supramolecular Chemistry: Concepts and Perspectives*, WILEY-VCH, Weinheim, 1995.

2 (*a*) M. Ruben, J. Rojo, F. J. Romero-Salguero, L. H. Uppadine and J.-M. Lehn, *Angew. Chem. Int. Ed.*, 2004, **43**, 3644; (*b*) B. H. Northrop, H.-B. Yang and P. J. Stang, *Chem. Commun.*, 2008, 5896; (*c*) M. Fujita, M. Tominaga, A. Hori and B. Therrien, *Acc. Chem. Res.*, 2005, **38**, 369; (*d*) B. J. Holliday and C. A. Mirkin, *Angew. Chem. Int. Ed.*, 2001, **40**, 2022; (*e*) S. J. Lee and W. Lin, *Acc. Chem. Res.*, 2008, **41**, 521.

3 (*a*) F. Puntoriero, S. Campagna, A.-M. Stadler and J.-M. Lehn, *Coord. Chem. Rev.*, 2008, **252**, 2480; (*b*) I. Eryazici, C. N. Moorefield and G. R. Newkome, *Chem. Rev.*, 2008, **108**, 1834; (*c*) I. Krivokapic, M. Zerara, M. L. Daku, A. Vargas, C. Enachescu, C. Ambrus, P. Tregenna-Piggott, N. Amstutz, E. Krausz and A. Hauser, *Coord. Chem. Rev.*, 2007, **251**, 364.

4 (*a*) E. C. Constable, *Coord. Chem. Rev.*, 2008, **252**, 842; (*b*) P. R. Andres and U. S. Schubert, *Adv. Mater.*, 2004, **16**, 1043; (*c*) Z. Shi and N. Lin, *J. Am. Chem. Soc.*, 2010, **132**, 10756; (*d*) R. Shunmugam, G. J. Gabriel, K. A. Aamer and G. N. Tew, *Macromol. Rapid Commun.*, 2010, **31**, 784.

5 (*a*) G. R. Newkome, T. J. Cho, C. N. Moorefield, G. R. Baker, M. J. Saunders, R. Cush and P. S. Russo, *Angew. Chem., Int. Ed.*, 1999, **38**, 3717; (*b*) G. R. Newkome, T. J. Cho, C. N. Moorefield, P. P. Mohapatra and L. A. Godínez, *Chem.–Eur. J.*, 2004, **10**, 1493; (*c*) S.-H. Hwang, P. Wang, C. N. Moorefield, L. A. Godínez, J. Manríquez, E. Bustos and G. R. Newkome, *Chem. Commun.*, 2005, 4672; (*d*) Y.-T. Chan, C. N. Moorefield, M. Soler and G. R. Newkome, *Chem.–Eur. J.*, 2010, **16**, 1768; (*e*) M. Soler, C. N. Moorefield and G. R. Newkome, *Adv. Heterocycl. Chem.*, 2010, **101**, 1.

6 S. Sakamoto, M. Fujita, K. Kim and K. Yamaguchi, *Tetrahedron*, 2000, **56**, 955.

7 C. A. Schalley, T. Müller, P. Linnartz, M. Witt, M. Schäfer and A. Lützen, *Chem.–Eur. J.*, 2002, **8**, 3538.

8 Y.-R. Zheng and P. J. Stang, *J. Am. Chem. Soc.*, 2009, **131**, 3487.

9 G. Hopfgartner, C. Piguet and J. D. Henion, *J. Am. Soc. Mass Spectrom.*, 1994, **5**, 748.

10 (*a*) B. T. Ruotolo, J. L. P. Benesch, A. M. Sandercock, S. J. Hyung and C. V. Robinson, *Nat. Protoc.*, 2008, **3**, 1139; (*b*) P. A. Faull, K. E. Korkeila, J. M. Kalapothakis, A. Gray, B. J. McCullough and P. E. Barran, *Int. J. Mass Spectrom.*, 2009, **283**, 140; (*c*) K. Thalassinos, M. Grabenauer, S. E. Slade, G. R. Hilton, M. T. Bowers and J. H. Scrivens, *Anal. Chem.*, 2009, **81**, 248; (*d*) G. R. Hilton, K. Thalassinos, M. Grabenauer, N. Sanghera, S. E. Slade, T. Wyttenbach, P. J. Robinson, T. J. T. Pinheiro, M. T. Bowers and J. H. Scrivens, *J. Am. Soc. Mass Spectrom.*, 2010, **21**, 845; (*e*) D. Smiljanic and C. Wesdemiotis, *Int. J. Mass Spectrom.*, DOI: 10.1016/j.ijms.2010.06.035.

11 (*a*) M. T. Bowers, *Science*, 1993, **260**, 1446; (*b*) C. S. Hoaglund-Hyzer, A. E. Counterman and D. E. Clemmer, *Chem. Rev.*, 1999, **99**, 3037; (*c*) S. Trimpin, M. Plasencia, D. Isailovic and D. E. Clemmer, *Anal. Chem.*, 2007, **79**, 7965; (*d*) B. C. Bohrer, S. I. Merenbloom, S. L. Koeniger, A. E. Hilderbrand and D. E. Clemmer, *Annu. Rev. Anal. Chem.*, 2008, **1**, 293.

12 (*a*) Y.-T. Chan, X. Li, M. Soler, J. L. Wang, C. Wesdemiotis and G. R. Newkome, *J. Am. Chem. Soc.*, 2009, **131**, 16395; (*b*) X. Ren, B. Sun, C. C. Tsai, Y. Tu, S. Leng, K. Li, Z. Kang, R. M. V. Horn, X. Li, M. Zhu, C. Wesdemiotis, W. B. Zhang and S. Z. D. Cheng, *J. Phys. Chem. B*, 2010, **114**, 4802; (*c*) S. Perera, X. Li, M. Soler, A. Schultz, C. Wesdemiotis, C. N. Moorefield and G. R. Newkome, *Angew. Chem., Int. Ed.*, 2010, **49**, 6539; (*d*) E. R. Brocker, S. E. Anderson, B. H. Northrop, P. J. Stang and M. T. Bowers, *J. Am. Chem. Soc.*, 2010, **132**, 13486; (*e*) X. Li, Y.-T. Chan, G. R. Newkome and C. Wesdemiotis, *Anal. Chem.*, 2011, **83**, 1284.

13 I. Eryazici, C. N. Moorefield, S. Durmus and G. R. Newkome, *J. Org. Chem.*, 2006, **71**, 1009.

14 Z. Bell, G. R. Motson, J. C. Jeffery, J. A. McCleverty and M. D. Ward, *Polyhedron*, 2001, **20**, 2045.

15 M. W. Cooke, P. Tremblay and G. S. Hanan, *Inorg. Chim. Acta*, 2008, **361**, 2259.

16 E. C. Constable, C. E. Housecroft, M. Neuburger, S. Schaffner and F. Schaper, *Inorg. Chem. Commun.*, 2006, **9**, 433.

 This journal is © The Royal Society of Chemistry 2011